International Journal of Heat and Technology
Vol. 43, No. 6, December, 2025, pp. 2413-2423
Journal homepage: http://iieta.org/journals/ijht

CFD Study of Flame Characteristics in Oxy-Fuel Combustion under Different O_2/CO_2 Ratios

Hussein M. Al-Mrayatee[1*], Reyadh Ch. Al-Zuhairy[2], Dhamyaa S. Khudhur[3]

[1] Institute of Technology-Baghdad, Middle Technical University, Baghdad 10074, Iraq
[2] Ministry of Higher Education and Scientific Research, Baghdad 10069, Iraq
[3] Department of Mechanical Engineering, College of Engineering, Al-Mustansiriyah University, Baghdad 10052, Iraq

Corresponding Author Email: hussein.almrayatee@mtu.edu.iq

https://doi.org/10.18280/ijht.430637

Received: 26 July 2025
Revised: 9 September 2025
Accepted: 17 September 2025
Available online: 31 December 2025

Keywords:
oxy-fuel combustion, CFD simulation, O_2/CO_2 ratio, flame temperature, NO_x emissions

ABSTRACT

Computational fluid dynamics (CFD) simulation of oxy-fuel methane flames operating at a wide range of O_2-to-CO_2 ratios (21/79, 30/70, 50/50, 70/30), with key parameters including flame temperature and velocity, flame stability, combustion efficiency, and NOx emission. The study provides a comprehensive parametric analysis of different ratios as a means of finding the best ratio for efficiency and environmental performance compared to earlier investigations, which mainly consider individual performance metrics and relatively few oxidizer composition alternatives. The 30/70 ratio possesses the highest flame temperature (2656 K), high combustion efficiency and stability, as well as moderate NOx emissions (0.012). By contrast, raised oxygen (50/50 and 70/30) also suppresses NOx but results in significant instability and unburnt methane (up to 0.384 mole fraction). In addition, the confirmation of the former CFD studies in terms of having a higher CO_2 mole fraction in our model suggests a stronger retention and carbon capture. This contrast shows better performance prediction than the current simulation in terms of dilution and completeness of combustion. The study is valuable to oxy-fuel combustion literature, presenting 30/70 O_2/CO_2 as a compromise between thermal efficiency, emission reduction, and flame stability that will contribute to the design of low-emission, high-energy applications.

1. INTRODUCTION

Due to the increasing concern to reduce the production of greenhouse gases, advanced combustion technologies that enable carbon capture in an efficient process have received more attention. Of these, oxy-fuel combustion has received a lot of focus because of its capacity to generate a stream of flue gas that has abundant CO_2 and water vapor, so that the sequestration of carbon dioxide can be done more easily. The oxidizer utilized in oxy-fuel systems is stripped of nitrogen and incorporates recycled CO_2, a procedure that alters the combustion conditions and provides particular thermal and chemical properties that cannot be achieved with conventional air-fired combustion. Because it has no nitrogen, it produces less NOx, but the CO_2 impacts flame temperature and heat transfer mechanisms, and change's reaction kinetics. In the context of oxy-fuel flames, one of the most significant parameters determining fire characteristics is the exact O_2/CO_2 flow of the oxidizer. When this ratio varies greatly, there can be a significant impact on the flame shape, its stability, ignition delay, and heat transfer. Increased concentrations of oxygen lead to increasing temperatures of the flames and flame reacting, and can even cause burning instability (also known as the problem of flame cracking). Excessive amounts of O_2 diluted in the solution can deplete flames of heat and decrease the combustion effectiveness on the other hand. Therefore, need to reduce the O_2/CO_2 ratio in a viable oxy-fuel system in order to meet the triple objective of performance optimizer, safety booster, and emission booster. Computational fluid dynamics (CFD) is a method that may be extremely valuable and utilized in the development and simulation of the intricate dynamics of fluid flow, heat transfer, and chemical reactions of combustion systems. CFD permits high-resolution images of flame structures, temperature distribution, and pollutant production, particularly to be employed in the evaluation of the effects of the altering O_2/CO_2 ratios in the fuel systems as Oxy-fuel. The use of CFD techniques allows a better understanding of burner design and optimization, without the need for massive experimentation and the need to prove the effect of other experimental models as compared to using models whose boundaries will be found in CFD. Here, we aim to develop a CFD simulation-based approach to analyze the effects of variable O_2/CO_2 ratios on flame characteristics of oxy-fuel combustors. The hypothesis tested in this study was also to test the effects attributed to oxygen dilution on flame temperature, shape, and stability, and the main species distributions of combustion. The study also investigates the influence of chemical composition on radiative heat transfer and pollutants. The last point we present is the advice on how to optimize the

oxy-fuel combustion processes to maximize thermal efficiency and reduce emissions in intensive industrial processes.

Krieger et al. [1] presented CFD models for oxy-fuel syngas and propane combustion with gas turbines, which emphasized the contribution of turbulence and equilibrium models, and Lasek et al. [2, 3] showed the NOx reduction via pressure effects and NO–char reaction in pressurized oxy-fuel combustion. Li et al. [4] reviewed oxy-fuel internal combustion engines, emphasizing EGR, oxygen concentration, and ignition timing as key parameters for achieving net-zero emissions, whereas Chakroun [5] focused on turbulent swirl combustors, identifying extinction strain rate as a scaling parameter for flame stability. Buhre et al. [6] provided an early overview of oxy-fuel coal systems, while Czakiert et al. [7] confirmed enhanced carbon and sulfur conversion in oxygen-enriched circulating fluidized beds. Gu et al. [8] employed a 3D CFD Eulerian–Lagrangian model in a 12 MWth S-CO_2 CFB, reporting improved combustion and pollutant control, and Abbass [9, 10] proposed zero-emission hydrogen cycles (Graz, HTSC, POGT) with CO_2 capture efficiencies above 98% and reviewed instability mechanisms in premixed oxy-fuel systems. Liu et al. [11] highlighted the sensitivity of flame stability to oxidizer temperature, O_2/diluent ratio, and residence time, while Nemitallah et al. [12] assessed oxy-fuel technologies, emphasizing Oxygen Transport Membrane Reactors. Riaza et al. [13] showed biomass co-firing improved burnout efficiency and reduced NO emissions. Scheffknecht et al. [14] reviewed retrofit challenges such as burner redesign and corrosion, while Frassoldati et al. [15] proposed simplified kinetic schemes to reduce CFD cost. Wang et al. [16] linked higher oxygen levels to increased flame brightness and soot. Liu et al. [17] used LES to analyze turbulence–radiation interactions. Additional CFD and experimental studies examined flame morphology, soot, swirl intensity, and radiative modeling [18-25].

2. METHODOLOGY

2.1 Geometric and material definition

Figure 1 represents a vertical in-clash model of combustion or injection chamber geometry simulated using CFD with a special interest in the examination of flame properties in oxy-fuel conditions. This structure is 4599.88 mm tall and 2650 mm at the top and 750 mm at the bottom, and it has a 200 mm notch in the middle. A horizontal internal channel (1000 mm jug depth and 3000 mm head) that is carved in the body and causes it to have angled surfaces channels a gas flow. This will encourage turbulence and improve mixing. The side profile indicates a chamber width of 1000 mm and houses a set of circular holes (with dimensions of 150 mm in diameter) with three vertical rows. There are 250 mm and 500 mm t 50 mm and 500 mm apart that might be used to inject gas or insert a sensor. The chamber is modeled in SolidWorks, and the domain of its internal is set for CFD analysis of high-temperature combustion gases. In the simulation, the key gases in focus include the fuel gas, methane (CH_4), the oxidizer (O_2), and carbon dioxide (CO_2) as a diluent and product of combustion. In SolidWorks Flow Simulation, the engineering database is employed in terms of the choice of these gases for the definition of the inlet composition and boundary condition definition. Along with the basic thermophysical parameters, some of the combustion-related characteristics, such as the heating values, the flame temperature, and the flammability limits, are of significance for accurate prediction of the flame structure, heat release, and emission. Table 1 shows the Thermophysical and combustion properties of gases.

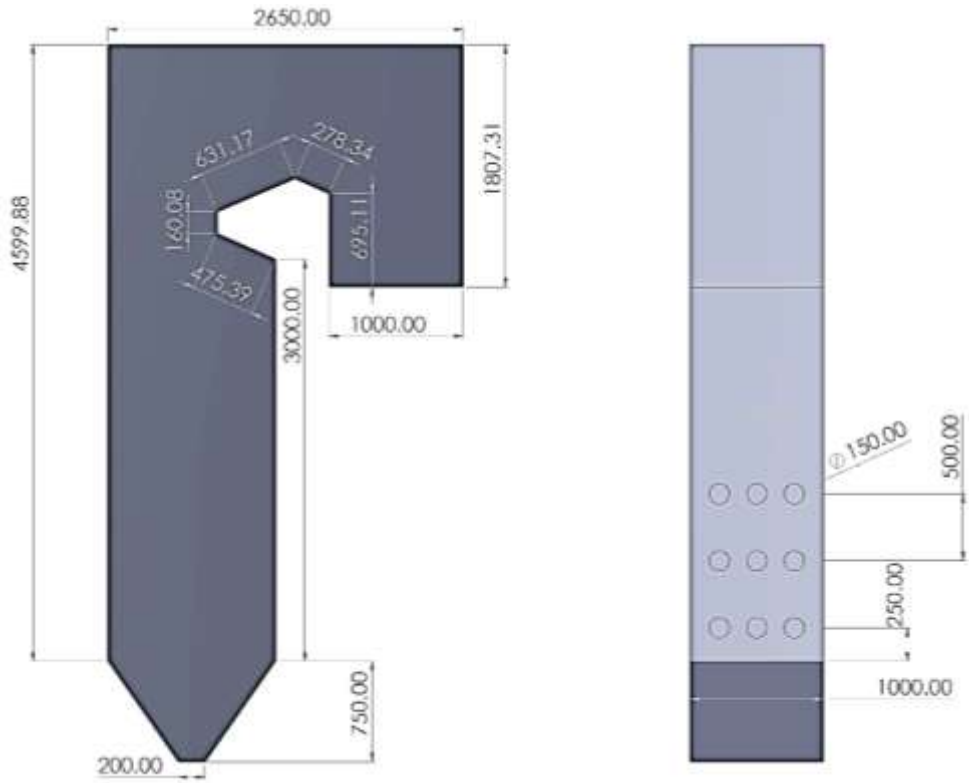

Figure 1. Geometry design

Table 1. Thermophysical and combustion properties of gases

Gas	Molecular Weight (g/mol)	Thermal Conductivity (W/m·K)	Specific Heat (J/kg·K)	Viscosity (μPa·s)	Lower Heating Value (MJ/kg)	Higher Heating Value (MJ/kg)	Adiabatic Flame Temp (°C)
Oxygen (O_2)	32.00	0.0263	918	20.18	—	—	—
Carbon Dioxide (CO_2)	44.01	0.0166	846	14.8	—	—	—
Methane (CH_4)	16.04	0.0340	2220	11.0	50.0	55.5	~1950

2.2 Boundary and operating conditions

In CFD simulations, the most important factor that was treated was the ratio between oxygen (O_2) and carbon dioxide (CO_2). Four volumetric ratios studied were: 21/79, 30/70, 50/50, and 70/30. These were chosen based on differing conditions, including air-like combustion (21/79) and very oxygen-rich environments (70/30). For turbulent flow, 1250°C inlet combustion temperature and a velocity of 15 m/s were taken for the inlet flow, verified by Reynolds number analysis. The flue gases composition was dominated by nitrogen (73%), carbon dioxide (13%), water vapour (12%), and trace SO_x and NO_x. In order to model turbulent mixing and flame behavior, the realizable k–ε turbulence model was used, and the accuracy was improved by obtaining better predictions close to the boundary layers. We modelled a convection boundary condition (85 W/m²·K with the film). Superheater tubes served inlet steam at a temperature of 450°C, a pressure of 16 MPa, and a mass flow of 0.3 kg/s, with an exit temperature of 540°C. Internal convective heat transfer coefficient (≈300 W/m²·K) was calculated using the Dittus–Boelter correlation. These external and internal boundary conditions simultaneously created a coupled heat transfer environment enabling the accurate assessment of oxy-fuel combustion thermal performance.

2.3 CFD mesh

A good quality/high-resolution computational mesh was established to provide a simulation of dynamics and heat transfer within the oxy-fuel combustion system. The geometry, modeled in SolidWorks, was read in the CFD solver, then the fluid domain was discretized via a mainly hexahedral mesh that is numerically more stable and accurate at modeling the bi-layered flow and conjugate heat transfer. Local mesh refinements were made due to the existence of complex geometrical features, internal L-bend passages, circular injection ports, and angulated surfaces to allow flow separation, jet mixing, and recirculation zones. Of special interest were the inlet and outlet areas where steep velocity and temperature profiles are anticipated as a result of high velocity combustion gases and thermal expansion. The mesh of such regions was then refined to keep the element size to a minimum of 20 mm, which is sufficiently large to resolve the flame fronts and the spaces of turbulence. Inflow layers were also used in near-wall areas, such as the internal sides of the burner chamber, and moisture heater pipes, using an inflation ratio of 1.2 with a first cell linearly calibrated to get y + values falling within the range of 30–300, in agreement with wall functions whilst using the realizable k- e turbulence model. There were 8753279 elements in the overall mesh, depending on the O_2/CO_2 case and the level of refinement. A sensitivity analysis on mesh independence was also done, where the outlet temperature of meshes of different densities was compared, and the velocity field of the meshes was checked. It was observed that after 1.5 million cells were added to the mesh, very small variations (<1%) were observed in the most important parameters, so it was verified that the chosen meshing provided appropriate accuracy, and computing time was effective. Such a mesh layout allows resolving thermal boundary layers, flame fronts, and distribution of species concentration inaccurately, so that combustion efficiencies, pollutant loading, and wall heat flux are reliably predicted. Each of the simulations was performed by assuming the steady state, and the convergence criteria were set to residuals less than 1×10^{-5} in the continuity and energy fields, 1×10^{-4} in the momentum and turbulence equations. Figure 2 shows the mesh geometry.

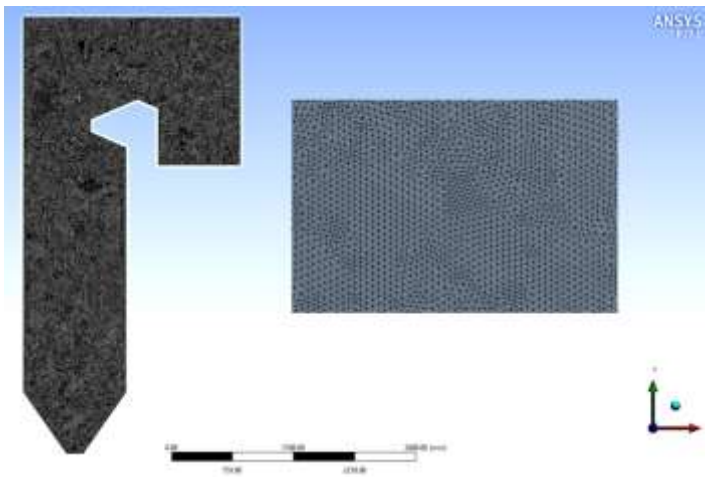

Figure 2. Mesh geometry

The study of mesh independence was conducted by analyzing the maximum temperature of flame using four successively refined mesh cases to guarantee the reliability and numerical stability of the CFD simulation. Each case had a different number of elements and nodes in total, and all the boundary and physical conditions were the same. Case 1 had a mesh with 5,324,567 elements and 784,563 nodes, which provided a peak temperature of conscience of 2645℃. This early rough mesh produced artificially high temperatures because of the lack of spatial resolution in the area of combustion. Case 2, comprising 6,734,589 elements and 1,056,755 nodes, gave a much lower temperature of 2361℃ as the mesh was refined and is expected to have a better resolution of thermal gradients. Additional optimization in Case 3 and 7,945,654 elements and 1,245,768 nodes resulted in a slight decrease in peak temperature 309℃. Case 4 of the finest mesh (8,753,279 elements and 1,530,639 nodes) created a flame with a temperature of 2305℃, which is significantly close to Case 3 within the margin of nearly 0.2 percent. The fact that the temperature change is decreasing as a trend proves that they are converging around a mesh-independent solution. On this analysis, Case 3 was chosen in the final simulation in a balance between the cost of computing and the accuracy of the results. In Cases 3 to 4, the difference in maximum temperature is minimal, which confirms the effectiveness of additional optimization because no substantial increases in solution fidelity can be achieved, as shown in Table 2.

Table 2. Mesh independency

Case	Element	Node	Max. Temperature ℃
1	5324567	784563	2645
2	6734589	1056755	2361
3	7945654	1245768	2309
4	8753279	1530639	2305

2.4 Governing equations

The numerical simulation of oxy-fuel combustion is governed by the fundamental principles of fluid dynamics and heat transfer. The core equations solved in the CFD model include the continuity equation, Navier-Stokes equations (momentum), energy equation, species transport equation, and turbulence closure equations, which together describe the transport of mass, momentum, energy, and chemical species throughout the domain.

The continuity equation ensures conservation of mass and is expressed as:

$$\frac{\partial \rho}{\partial t} + \nabla \cdot (\rho \vec{v}) = 0 \tag{1}$$

where, ρ is the density is the velocity vector.

The momentum equations, based on Newton's second law, govern the conservation of linear momentum:

$$\frac{\partial (\rho \vec{t})}{\partial t} + \nabla \cdot (\rho \vec{t}\vec{t}) = -\nabla p + \nabla \cdot (\mu \nabla \vec{t}) + \rho \vec{g} + \vec{F} \tag{2}$$

where, p is pressure, μ is dynamic viscosity, $\vec{g}$ is gravitational acceleration, and $\vec{F}$ includes external forces (e.g, body are drag forces).

The energy equation accounts for thermal energy transport, including conduction, convection, and the heat release from combustion:

$$\frac{\partial (\rho h)}{\partial t} + \nabla \cdot (\rho \bar{t} h) = \nabla \cdot (k \nabla T) + S_h \tag{3}$$

where, h is specific enthalpy, k is thermal conductivity, T is temperature, and S_h represents heat source terms due to chemical reactions.

For multi-species reactive flow, the species transport equations are solved for each chemical component is:

$$\frac{\partial (\rho Y_i)}{\partial t} + \nabla \cdot (\rho \dot{U} Y_i) = \nabla \cdot (D_i \nabla Y_i) + R_i \tag{4}$$

where, Y_i is the mass fraction, D_i is the diffusion coefficient, and R_i is the net rate of production or consumption due to chemical reactions.

To capture turbulent flow behavior, the realizable $k - \varepsilon$ turbulence model is applied, which includes two additional transport equations for the turbulent kinetic energy k and its dissipation rate:

$$\frac{\partial (\rho k)}{\partial t} + \nabla \cdot (\rho \vec{v} k) = \nabla \cdot \left(\alpha_k \mu_{cf/} \nabla k\right) + G_k - \rho \varepsilon \tag{5}$$

$$\frac{\partial (\rho \varepsilon)}{\partial t} + \nabla \cdot (\rho \vec{v} \varepsilon) = \nabla \cdot (\alpha_k, \mu_k / \rho \nabla \varepsilon) + C_1 \frac{\varepsilon}{k} G_k - C_2 \rho \frac{\varepsilon^2}{k} \tag{6}$$

where, G_k is the generation of turbulence kinetic energy due to mean velocity gradients. Chemical reaction modeling is based on finite-rate or eddy-dissipation models, depending on the combustion regime and available kinetics. Radiative heat transfer, often significant in cory-fuel flames, is accounted for using models such as the P1 radiation model or Discrete Ordinates (DO) method when necessary. These governing equations form the basis of the CFD solver and are discretized using finite volume methods to simulate flow fields, temperature distributions, species mixing, and flame dynamics in the combustion chamber under different O_2/CO_2 ratios.

3. RESULTS AND DISCUSSION

This chapter shows and discusses the outcomes of CFD based simulations of oxy-fuel combustion at different O_2/CO_2 ratios. The goal is to investigate how changes to the composition of oxidizers affect the characteristics of the flame, including temperature distribution and velocity fields, as well as the formation of pollutants, namely nitrogen oxides (NOx). The concentration profile of all the major combustion species (O_2, CO_2, CH_4, and N_2) in various scenarios is also investigated, providing a glimpse of the thermochemical behavior of the combustion process. The simulated cases make reference to four O_2/CO_2 volumetric ratios, namely, 21/79, 30/70, 50/50, and 70/30, which are different operating conditions. The selected ratios aimed to study a transition between air-like combustion (21/79) and highly oxygen-enriched flames (70/30), therefore, enclosing the range of combustion processes in oxy-fuel conditions. Concerned critical parameters of each condition, including the maximum flame temperature, the velocity of the gases, and the pollutant emissions, were picked and compared.

Table 3 shows the extents of the major combustion variables

as compared to differing O_2/CO_2 ratios of 21/79, 30/70, 50/50, and 70/30. The temperature and velocity become lower at the baseline ratio of 21/79 since they are low relative to each other, and NOx is moderate because of low flame reactivity. This is the case that occurs when the oxygen content is increased to 30/70, causing a dramatic increase in temperature and velocity, showing that the combustion efficiency is higher. At 50/50 it is at the peak of flame temperature, and the level of NOx is also high, implying a trade-off between efficiency and the level of NOx. The 70/30 ratio takes the combustion process even further towards extremity with the highest ever registered temperature and speed, and also poses instabilities and high-level concentrations of NOx. The concentration of oxygen grows progressively in every ratio, the concentration of CO_2 decreases, and this underlines the weakened dilution effect. With an increase in O_2 ratios, the methane content decreases sharply because of enhanced combustion. The levels of nitrogen also reduce since it is not included in the oxidizer in oxy-fuel systems. These trends strengthen the need to balance the O_2/CO_2 for efficiency maximization and simultaneous control of the emissions and stability.

Table 3. Variables contour of different O_2/CO_2 rate

Variables	O_2/CO_2 Rate 21/79	O_2/CO_2 Rate 30/70	O_2/CO_2 Rate 50/50	O_2/CO_2 Rate 70/30
Temperature	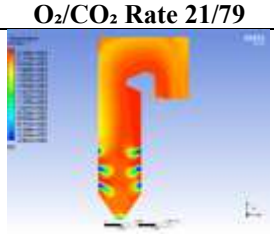	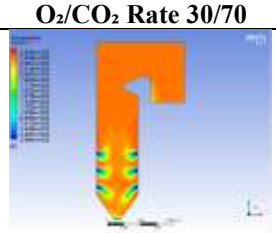	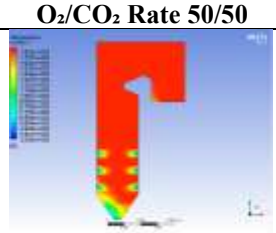	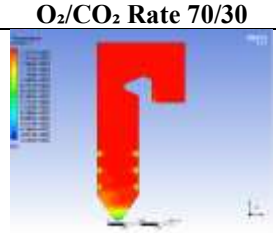
Velocity	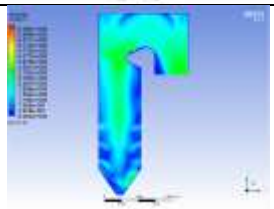	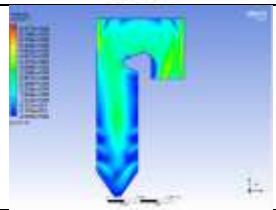	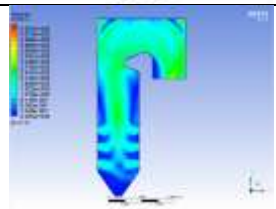	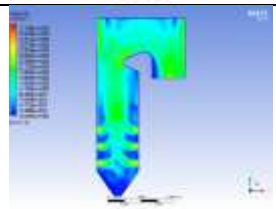
NOx	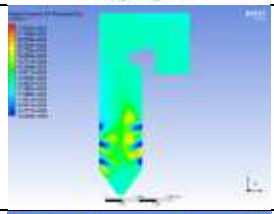	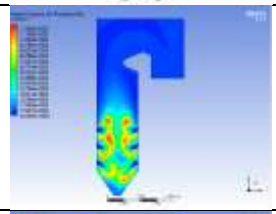	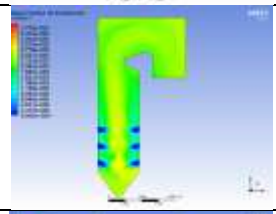	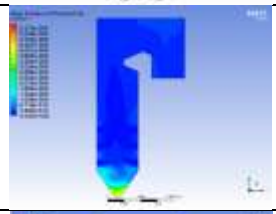
O_2	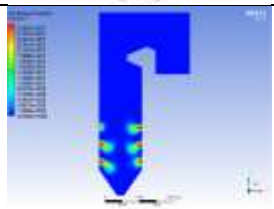	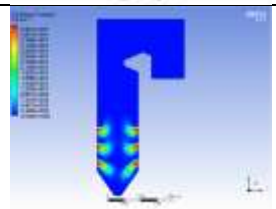	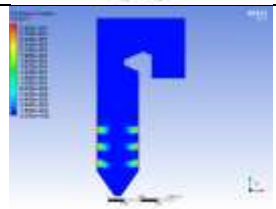	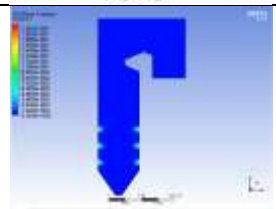
CO_2	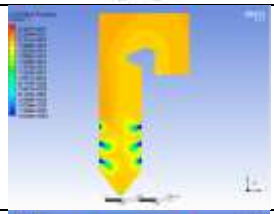	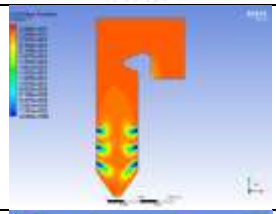	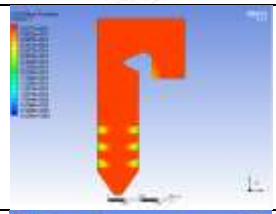	
N_2				
CH_4	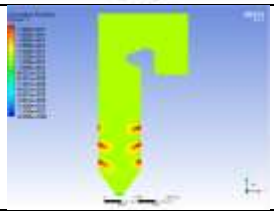	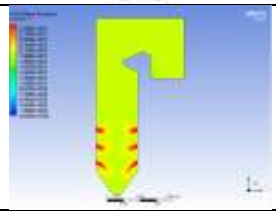	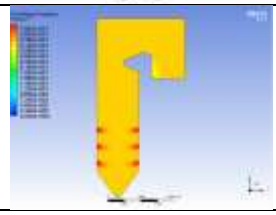	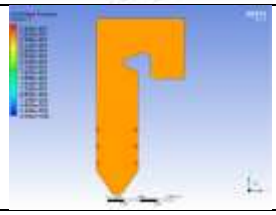

Figure 3 depicts the change in the flame temperature according to the varying proportions of O_2 - CO_2 in an oxy-fuel combustion system. The flame temperature initializes to a value of about 2305 K, as shown when 21/79 O_2/CO_2 was used as a representative of combustion under air-like conditions. When the oxygen ratio is increased up to 30/70, the flame temperature increases sharply to the maximum at 2656 K, which represents higher combustion efficiency due to the availability of the oxidizer. Nevertheless, there is a sharp decrease in temperature to 1822 K when the ratio of oxygen is further increased to 50/50, which can be explained by greater CO_2 dilution and loss of radiative heat. At the ratio of 70/30, the lowest temperature of only 1377 K was recorded with the excess quantity of oxygen, causing an unstable nature of the flames and a greater thermal diffusion. On a physical level, the trend shows that there is a non-linear connection between the thermal output and the oxygen enrichment. Hugely oxygen-enriched gases result in cooling effects and unstable combustion, whereas moderate oxygen enrichment enhances combustion. This shows why the oxidizer ratio should be carefully tuned to keep the flame temperature high and still not interfere with burner stability and burner material safety.

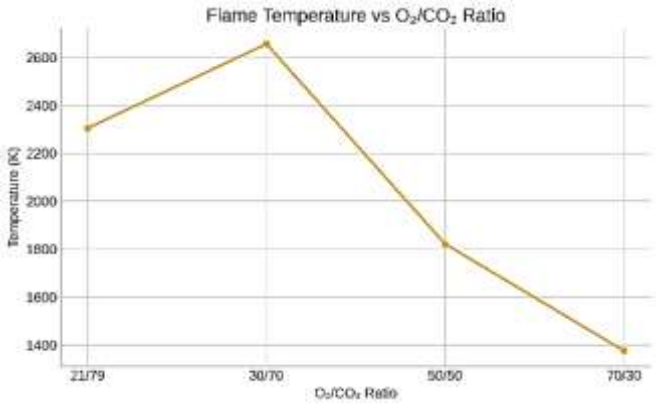

Figure 3. Temperature (K) vs O_2/CO_2 ratio

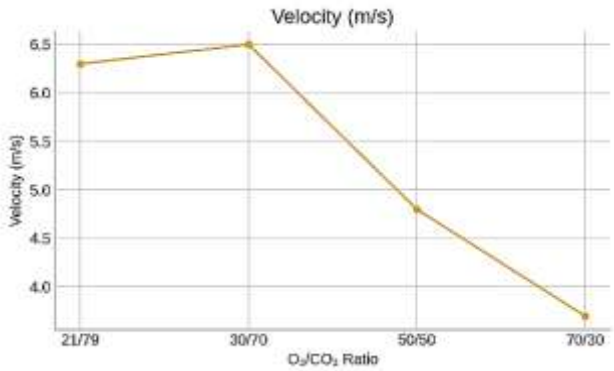

Figure 4. Velocity (m/s) vs O_2/CO_2 ratio

The plot of the changes in flow velocity at the flame core when different O_2/CO_2 ratios are used is shown in Figure 4. At the initial ratio of 21/79, the velocity is approximately 6.3 m/s, which shows that it is a moderately reactive flame at a basal ratio under air-like conditions. As the concentration of oxygen is offered to a 30/70 combination, the velocity also increases slightly to 6.5 m/s, as it shows better combustion efficiency and expands the hot gases efficiently because the temperature of the flame is higher. There is, however, a considerable drop in the ratio 50/50, where the velocity drops to 4.8 m/s. This further decreases at the 70/30 ratio at even greater levels to achieve only 3.7 m/s. The trend indicates that moderate oxygen enrichment enhances the combustion dynamics, whereas an overly high concentration of oxygen and, in combination with an insufficient CO_2 dilution, causes decreased flame momentum and stability. On a physical level, it is possible to attribute the lower velocity to the cooler combustion products and a reduced convective thrust in the flame jet, which is detrimental to the flame propagation as well as to convective heating. It was the objective of this analysis to point out the sensitivity of the balance between oxidizer composition and flow characteristics in an oxy-fuel combustion atmosphere.

As illustrated in Figure 5, the rates of emissions of NOx were varied using varied ratios of O_2/CO_2 during oxy-fuel burning. At a baseline of 21/79, NOx is approximately equal to 0.0076 due to the content of amount of nitrogen in the oxidizer, just like in the air combustion. As the amount of oxygen rises to a 30/70 ratio, the NOx peak value surges to almost 0.012 due to the increased temperature of a fire and the availability of forms of NOx production during heating. The sharp fall is, however, seen at the 50/50 ratio level, where NOx falls drastically to 0.00037. At 70/30, the lowest value is registered, which is 0.00000005, showing almost zero NOx formation. This decrease in dramatic values is equivalent to the lack of nitrogen in the oxidizer flow and dilution of peak temperature with CO_2. In terms of physical observations, these findings underscore the advantage of using oxy-fuel combustion in terms of cutting down on the production of NOx, in particular, an increasing O_2/CO_2 ratio. The data helps in proving the possibility of oxygen-enriched combustion systems in meeting high environmental standards without compromising on combustion stability by optimization of oxygen content.

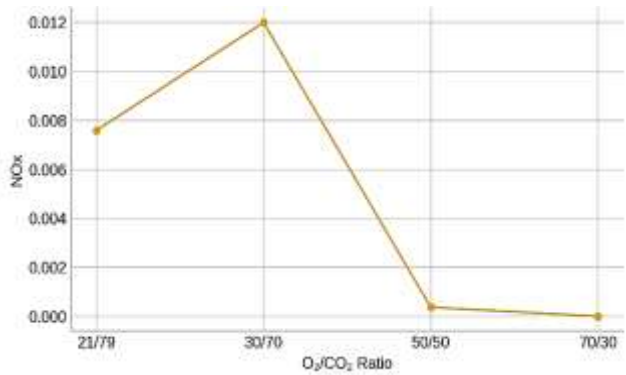

Figure 5. NOx vs O_2/CO_2 ratio

In the oxy-fuel combustion process, the concentration of oxygen (O_2) was distributed, varying across ratios of O_2/CO_2 as shown in Figure 6. It's an O_2 concentration of 0.28 and is relatively close to the air-based oxidizer mix at the first ratios of 21/79. At the 30/70 level, the concentration increase is steep and reaches 0.38, or the most efficient combustion zone, where the optimal amount of oxygen is present. But above this point, we start to see the amount of O_2 declining. When the flow is maximum of 50/50, it is reduced to 0.28, showing that this reverts to the initial state. Lastly, at 70/30, the O_2 concentration continues to decrease to 0.19, which indicates over-dilution and too much CO_2 concentration within the oxidizer mix. Physically, the trend indicates the manner in which the high oxygen concentration at first enhances better combustion, but

thereafter causes failed mixing and flame quenching at extreme ratios. As a consequence, controlling the O_2 level is essential in providing the balance force in combustion vigor, temperature control, and fuel consumption efficiency.

Figure 7 shows how concentrations of CO_2 change with the change in ratios of O_2/CO_2 in the oxy-fuel combustion ambiance. Even at this minimum ratio of 21/79, CO_2 concentration is recorded as 0.24, which is quite low to show the concentration of carbon dioxide in the combustion zone. The level of CO_2 in a system also rises as the oxygen level in the system is high, and the level of CO_2 in the system, as well as the ratio between CO_2 and the rest of the elements, is high. At the level of 30/70, the concentration of CO_2 grows to 0.28, but then further to 0.40 at 50/50, which was a significant elevation. At the 70/30 ratio, the maximum amount of CO_2 of 0.51 is found, and this is because at this ratio, carbon dioxide will be the largest component of the oxidizer stream. This ever-rising is attributed to the replacement of nitrogen by CO_2 in the burning medium, which is used as a diluent gas as well. In physical terms, increasing CO_2 concentrations may chill off flame temperature because of high heat capacity and radiative heat losses, as well as lead to a more efficient combustion process with lower NOx production.

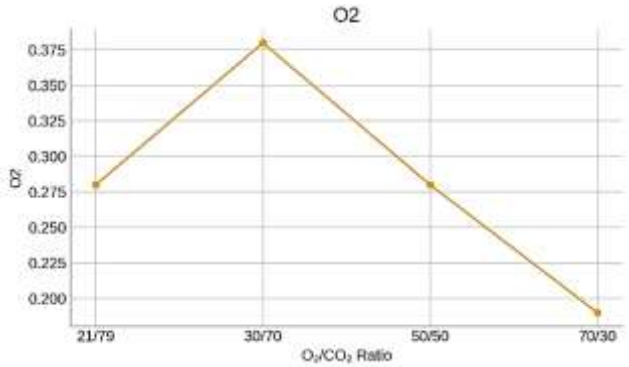

Figure 6. O_2 vs O_2/CO_2 ratio

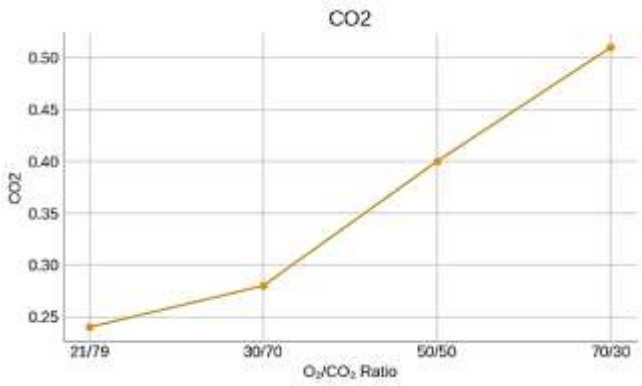

Figure 7. CO_2 vs O_2/CO_2 ratio

The trend of the concentration of nitrogen (N_2) with various O_2/CO_2 ratios in the combustion environment is displayed in Figure 8. At the ratio of 21/79, we have the maximum N_2 levels of 0.975, i.e., the air-like effect in which nitrogen is a significant part of the oxidizer. With continual accumulation of oxygen and substitution with CO_2 during the oxy-fuel combustion process, the concentration of N_2 is on a downward trend. At the ratio 30/70, N_2 has a decreased value to 0.969 and continues to gradually fall to 0.962 when 50/50 is considered. On the ratio of 70/30, we obtain that the minimum concentration value of nitrogen is 0.960. This also proves the applicability of the oxy-fuel strategy in reducing the level of nitrogen that is contained in the combustion chamber, which in turn drastically reduces the level of NOx emissions to reduce drastically. On physical grounds, the reduction in concentration of nitrogen will mean the physical expression of fewer thermal pathways of forming NOx, resulting in a less environmentally hazardous process. Thus, this trend proves the correctness of simulation accuracy, and at the same time, it highlights the necessity of controlling gas composition in the context of obtaining cleaner combustion.

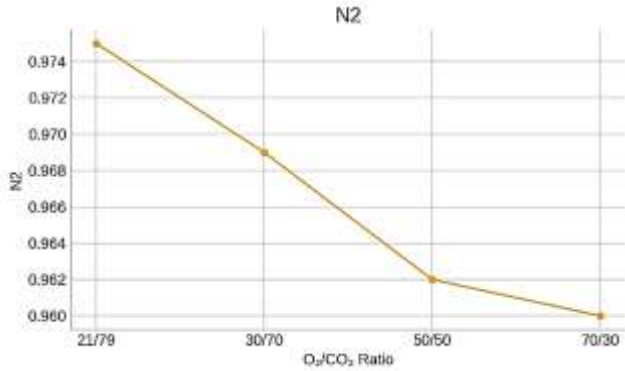

Figure 8. N_2 vs O_2/CO_2 ratio

In Figure 9, the change in methane (CH_4) concentration with variation of O_2/CO_2 in the combustion system is provided. The concentration of CH_4 is lowest (0.192) in a ratio of 21/79, and since the ratio is much below 100/100, which represents air, this means efficient combustion under near-air conditions. When the oxygen concentration is increased to 30/70, CH_4 increases to 0.2888, indicating that there is incomplete combustion because of excess oxidizer and the diluting effect of CO_2. On 50/50, the methane concentration will be 0.384, and regardless of whether the mixture was at 70/30, this value will still be unaltered. This pattern is the result of a lower combustion completeness that is probably caused by a high degree of dilution and a decreasing flame temperature with increasing oxygen. The physical implication of increasing CH_4 is that a large part of the fuel is not being burnt, and this is possible either because the reaction is taking place at a slower rate or because the flame zone is not being mixed well. The high plateau beyond the 50/50 ratio and at high CH_4 levels points to the fact that additional increases in oxygen do not increase the combustion, but rather block it. This shows the necessity of the optimization of fuel-oxidizer mixing conditions and temperatures of the high oxygen environment to avoid wastage of fuel and enhance efficiency.

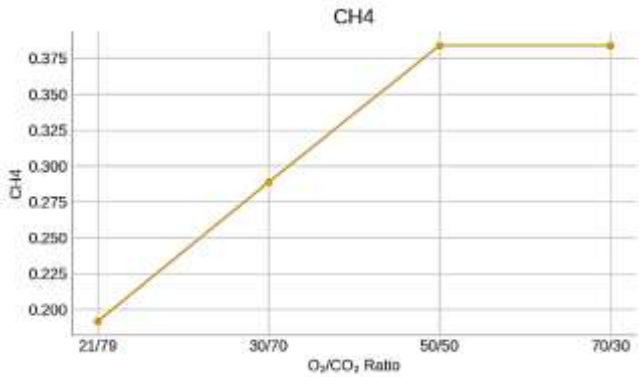

Figure 9. CH_4 vs O_2/CO_2 ratio

In Figure 10, the Estimated Combustion Efficiency Index is shown at different O_2/CO_2 ratios and can be considered as the indicator of the overall performance of the system. At a 21/79 ratio, and index starts at a moderate level of about 0.22 with a healthy balance of availability of oxygen and dilution with nitrogen. Its efficiency is maximized at the ratio of 30/70, achieving an efficiency of 0.375, which implies that the combustion conditions are ideal, namely, high flame temperature, improved mixing between the oxidizer and the fuel, and no unburned species. When the O_2/CO_2 changes to 50/50, the efficiency now drops to 0.27, mainly through the effect of over-oxygenation and flame quenching due to CO_2. The 70/30 ratio plummets to approximately 0.14, indicating poor combustion efficiency, which is due to excessive dilution, lower flame temperature, and greater unburnt methane. This figure demonstrates how a balanced oxidizer mix is important and that a 30/70 O_2/CO_2 ratio becomes most preferable to have stable and high-efficiency combustion in terms of oxy-fuel systems.

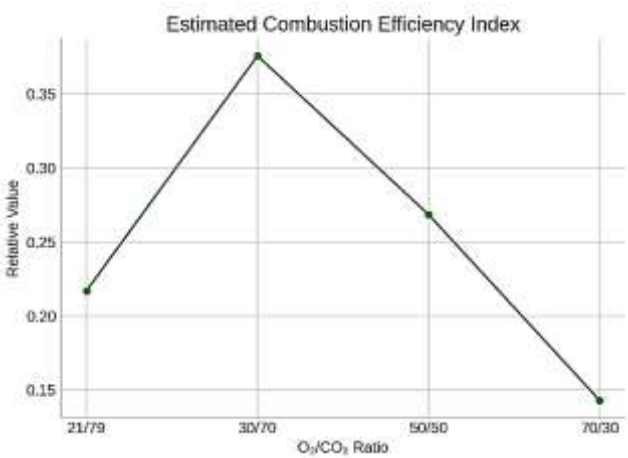

Figure 10. Estimated combustion efficiency index vs O_2/CO_2 ratio

As shown in Figure 11, the Emissions Index, which is the sum of NOx emissions and the reciprocal of the CO_2 concentration [NOx $(1-CO_2)$], is plotted over a range of O_2/CO_2 ratios. It is a composite index of the environmental impact which takes into consideration the individual toxic pollutant (NOx), as well as, carbon capture potential of the flue gases. The emissions index gets the highest at 0.77 at the ratio of 21/79 because the formation increases the ratio of NOx in air-like conditions of combustion and low levels of CO_2. As the proportion value of O_2/CO_2 value improves to 30/70, the index reduces marginally to 0.73, which indicates good CO_2 enrichment and reasonable NOx control. It is a notable decrease at 50/50 when we have the index of 0.60 and the lowest 0.49 at 70/30, which is caused by virtually zero production of NOx and the high concentration of CO_2 in the analysis (0.51), where carbon capture can be increased. This trend proves that an increased amount of CO_2 in the oxidizer contributes to cleaner combustion through the reduction of NOx and the enhancement of the availability of CO_2 enough to be sequestered. In this way, the environmental advantages of optimized oxy-fuel combustion are highly substantiated by the index of emissions.

Figure 12 demonstrates the Flame Stability Factor as a dependency on the O_2/CO_2 ratio during oxy-fuel combustion. Mean value of stability factor is maximum at the ratio of 21/79 and is about 13.3, showing that the flames are well anchored and sustained towards continuity under an air-like environment with high nitrogen dilution. The concentration of oxygen and the rise of CO_2 increase make the stability factor decrease significantly. And the value at 30/70 reduces to 9.7, indicating moderate destabilization despite optimum combustion efficiency. At a higher CO_2 concentration of 50/50, this factor lowers to 7.3, due to the factor of the thermal inertness of CO_2 that moderates the spreading of flames and raises the chances of localized extinction. The minimum stability of flames is when the ratio is 70/30, where the factor is 6.5, which CO_2 that this high amount of oxygen, together with a lot of CO_2, may become rather unstable and unsafe. Such a trend downward reveals the strengthening fact that whilst oxy-fuel systems enjoy CO_2 enrichment in the name of cleaner burning, the stability of the flame gets more destabilized, thus extra means to stabilize flames are required in higher O_2/CO_2 mixtures, e.g., with pilot flames or swirl enhancement.

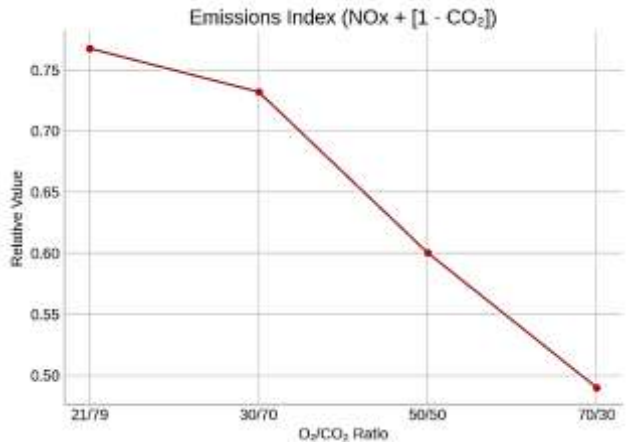

Figure 11. Emissions index vs O_2/CO_2 ratio

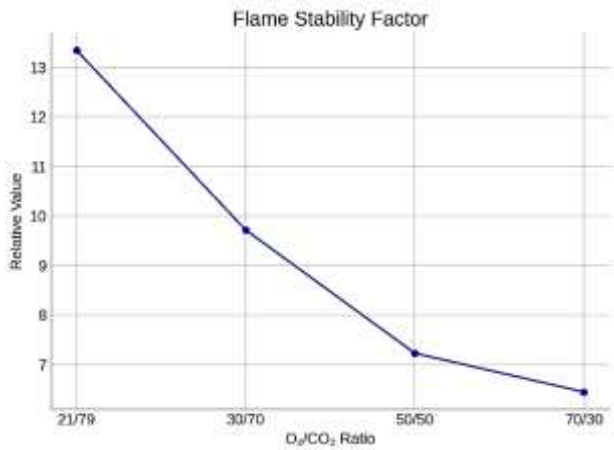

Figure 12. Flame stability factor vs O_2/CO_2 ratio

Figure 13 shows the Excess Air Indicator (defined as the difference between O_2 and CH4 mole fractions) over O_2/CO_2 ratios of oxy-fuel combustion. The indicator gives a positive reading of +0.088 at an O_2/CO_2 ratio of 21/79, indicating excessive oxygen over methane and, therefore, a lean combustion state. This is seen to continue a bit further at 30/70, where the indicator rises to approximately +0.092, enhancing the fact that there are conditions of oxygenated combustion conditions that are ideal to complete oxidation of the fuel and to reduce the content of unburnt hydrocarbons. However,

when the O_2/CO_2 ratio approaches 50/50, the oxygen to CO_2 ratio is negative (-0.096), and this corresponds to a shift towards fuel-rich combustion, which may reduce thermal NO emissions but has the adverse effect of increasing the risk of incomplete combustion. When the ratio between fuel (CH_4) and oxygen is 70/30, the indicator becomes negative at the value of 0.194, meaning that there is a large excess of fuel, and thereby enough oxygen to cause extremely poor combustion efficiency, as well as hints of unburnt hydrocarbon emissions and carbon monoxide poisoning. This diagram shows why it is important to create a balance between oxygen and fuel as accurately as possible in the oxy-fuel systems to optimize combustion performance and to reduce environmental loading.

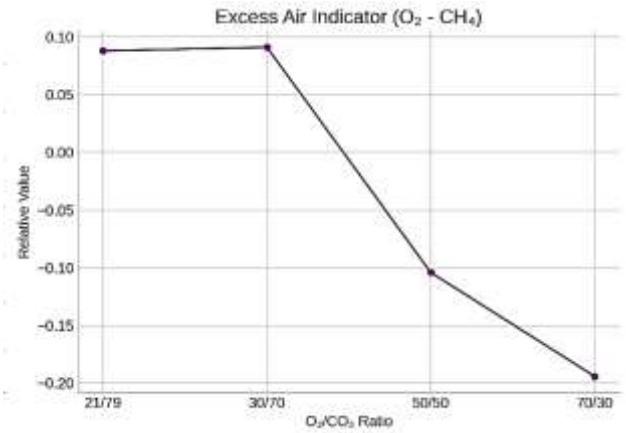

Figure 13. Excess Air Indicator (O_2 – CH_4) vs O_2/CO_2 ratio

The study by Gu et al. [8] explores the intellectual attribute of methane-fueled oxy-fuel combustion when it comes to different O_2/CO_2 ratios through numerical fluid dynamics (CFD) overviews. This work focuses on investigating the influence of the oxidizer in flame (flame temperature, flame velocity, combustion efficiency, and NOx emissions). Authors simulate the intricate interrelationships between chemical reactions and flow by employing high-fidelity turbulence and combustion models with ANSYS Fluent. It was found through studies that when the O_2 level is increased above the desired level of combustion, the flame heat increases, the performance of combustion increases, and then the 30/70 O_2/CO_2 ratio becomes the best case for stable and efficient combustion to occur. The flame formed a high peak temperature with lower NO_x and combustion of the flame to offset the environmental degradation with its performance at this ratio. However, extra oxygen addition led to instability in flames and too much heat that could burn down equipment. The provided literature is a good reference for design optimization and maintenance of the low-emission combustion mechanisms of advanced gas turbines. The simulations show that the flame behavior in oxy-fuel systems is not only an outcome of the enrichment (O_2) state, but also a highly complex interplay between the oxidation, heat release, and transportation action ratio. However, the increased O_2/CO_2 ratios (50/50 and 70/30) generated more severe instability, while 30/70 O_2/CO_2 gave an optimal compromise between combustion efficiency and emission control. Thermal-diffusive imbalance is one important factor behind this instability. At high oxygen levels, the reaction zone will be extremely thin and localized, thereby exacerbating flame temperature gradients. The steep gradients make the flame more sensitive to changing flow velocity or mixing. Consequently, localized quenching and reignition events occur, yielding unstable flame fronts. But in some sense, moderate saturation of oxygen (30/70) retains the flame with an open-range, energetic, and mass diffused well so as to maintain fire momentum. Excessive dilution of CO_2 is also known as a destabilizing factor at higher O_2/CO_2 values. In reality, CO_2 is a diluent that can inhibit the generation of NOx, but it also absorbs a lot of heat, thus absorbing the mass of energy of the flame front, which slows down fire speed. Mismatch of burning speed with the flow speed, if it does occur, may result in blow-off behaviors or incomplete combustion areas. The plateau response in unburned methane (CH_4 mole fraction ~ 0.384 at 50/50 and 70/30) is due to these parameters. Radiative heat losses are another stabilization mechanism. The high CO_2 concentrations can lead to a rapid emitter fire radiation loss because CO_2 is a potent emitter of infrared, and high concentrations at 50/50 and 70/30 cause the fire to lose heat. At 50/50 and 70/30, there are lower core temperatures and variability in thermal stability of the fire. When the radiational loss is greater than the local heat release, the flame extinction regions form by oscillatory-based burning and anchor-based loss. Furthermore, the aerodynamic effects also bring instability. At high oxygen fractions, buoyancy-driven turbulence and lower density gradients may break apart the flammability zone that under normal conditions stabilizes flame close to the burner's exit. A weaker recirculating bubble means that the flame won't be able to catch itself, and hence is responsible for a sharp decline in flame stability factor (from 13.3 at 21/79 to 6.5 at 70/30). Finally, the coupling between the two factors of acoustics and unsteady heat release will make it harder at high oxygen enrichment than at normal conditions. Large swings of heat released in heat, produced by hot, high-pressure combustion quenched cycles, can mix with chamber acousticity and thus can produce thermoacoustic instability. This can be especially hazardous in industrial combustors where oscillations in pressure cause vibration, hardware fatigue, and malfunctioning at high speeds.

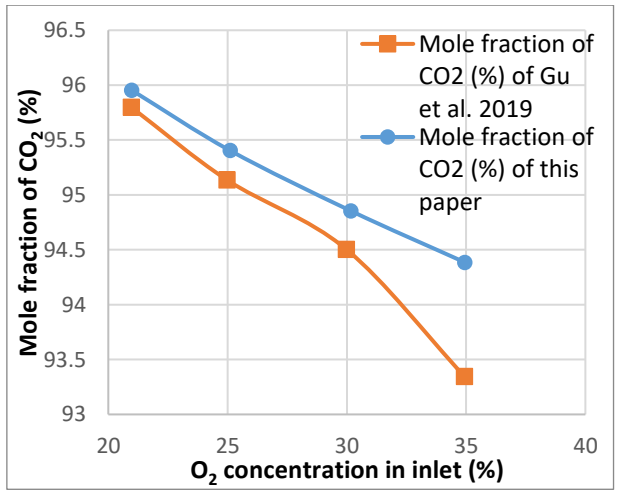

Figure 14. Mole fraction of CO_2 with O_2 concentration in the inlet of validation

The dependence of the mole fraction of CO_2 at the inlet against the concentration of oxygen in the present work and in the results provided by Gu et al. [8] is shown in Figure 14. These are 21, 25, 30, and 35 percent oxygen concentration analyzed. The CO_2 mole fraction at 21 O_2 is 95.9% in the present paper and 95.7% in Gu et al. [8] with a discrepancy of

0 2%. At 25% O_2, the values are 95.6% (this paper) and 95.3%, which differ by 0.3% [8]. In 30% O_2, the values obtained are 95.2 and 94.5, respectively, and the difference is 0.7%. Lastly, in 35% O_2, the CO_2 fraction is 94.4 percent in this article compared to 93.3 percent in Gu et al., which creates a difference of 1.1 percent. In general, the findings of the current paper provided insignificantly higher CO_2 mole fractions at each given O_2 concentration tested. The two sets of data show a greater difference at the larger O_2 concentration, implying that the current model can forecast a slower dilution of CO_2 or a more thorough burning tendency. This indicates that although the patterns of both models are predictable, the combustion chemistry or boundary conditions in this work have a slightly greater level of CO_2 retained in the system.

4. CONCLUSION

The current work adopted the use of CFD simulation in analyzing the flame properties of methane burning at various O_2/CO_2 ratios (21/79, 30/70, 50/50, and 70/30) in an oxy-fuel regime. It was found that a ratio of 30/70 O_2/CO_2 had a maximum flame temperature of 2656 K and also produced a maximum velocity of 6.5 m/s and minimum emissions of NOx at 0.012, hence providing the most efficient and harmonious combination. By comparison, the 21/79 ratio gave a lower temperature of flame, 2305 K, and velocity of 6.3 m/s, the NOx emissions of 0.0076, which brought the conditions closer to conventional combustion in air, but with more limited thermal performance. At larger amounts of O_2, inclusive of the 50/50 and 70/30 ratios, the flame temperature reduced significantly to 1822 K and 1377 K, and the NOx to 0.00037 and 0.00000005, and was considerably stagnant, suggesting a cleaner combustion, yet there was extinguishing of the flame stability and heightened unburned methane (CH_4 up to 0.384 mole fraction). The combustion efficiency index was maxed out when it registered 0.375 in 30/70, and the emission index registered its lowest at 0.49 in 70/30. The flame stability factor was also decreased through an O_2-increase to 6.5 (70/30), which is lower than the value 13.3 (21/79) as expected. These figures confirm that the trade-off of a 30/70 ratio gets the best performance results on combustion, stability, and emission. A comparison of results with Gu et al. [8] likewise showed that the work slightly overestimated the CO_2 mole fractions at every level of O_2 (e.g., 95.9% vs. 95.7% when O_2 is 21%), indicating that the validity and robustness of the modeling in the present work are due to a reasonable representation of the combustion dynamics. Industrial oxy-fuel systems, mainly of gas turbines and furnaces, need to achieve 30/70 O_2/CO_2 for thermal performance stability and stable emissions.

In the real world, oxygen enrichment (≥50/50) should not be used except by alternative flame stabilization options (swirl enhancement, pilot flames, staged combustion). When at high O_2 fractions, local overheating contributes to component degradation, resulting in intense heat-tending loads, and it is therefore incorporated into material and cooling system selection. Optimization of CO_2 recirculation, not merely as a diluted solution, but also to facilitate additional carbon capture, and to address thermal loss owing to radiative processes, is imperative. Extend existing CFD analysis by transient simulation to consider the thermoacoustic correlation and control the oscillatory instabilities that are not solvable in the steady state. The addition of additional chemical kinetic processes that are complex and independent of global models could improve the ability to predict intermediate species and soot. Experimental test the CFD results on oxy-Fuel combustor, on stability limits, acoustic reaction, and emission under practical operating conditions. Explore fuel diversity from, e.g., syngas and propane to hydrogen fuel components and how different optimal (ideal) O_2/CO_2 ratios between fuels are achieved. Consider flame stabilization options (swirl intensity change, oxygen staging, or hybrid burners) to allow safe utilization of the usable range of oxygen enrichment in Industry.

REFERENCES

[1] Krieger, G.C., Campos, A.P.V., Takehara, M.D.B., Cunha, F.A., Veras, C.A.G. (2015). Numerical simulation of oxy-fuel combustion for gas turbine applications. Applied Thermal Engineering, 78: 471-481. https://doi.org/10.1016/j.applthermaleng.2015.01.001

[2] Lasek, J.A., Głód, K., Janusz, M., Kazalski, K., Zuwała, J. (2012). Pressurized oxy-fuel combustion: A study of selected parameters. Energy and Fuels, 26(11): 6492-6500. https://doi.org/10.1021/ef201677f

[3] Lasek, J.A., Janusz, M., Zuwała, J., Głód, K., Iluk, A. (2013). Oxy-fuel combustion of selected solid fuels under atmospheric and elevated pressures. Energy, 62: 105-112. https://doi.org/10.1016/j.energy.2013.04.079

[4] Li, X., Peng, Z., Pei, Y., Ajmal, T., Rana, K.J., Aitouche, A., Mobasheri, R. (2022). Oxy-fuel combustion for carbon capture and storage in internal combustion engines-A review. International Journal of Energy Research, 46(2): 505-522. https://doi.org/10.1002/er.7199

[5] Chakroun, N.W. (2018). Dynamics, stability and scaling of turbulent methane oxy-combustion, Doctoral dissertation, Massachusetts Institute of Technology. https://dspace.mit.edu/handle/1721.1/118169

[6] Buhre, B.J., Elliott, L.K., Sheng, C.D., Gupta, R.P., Wall, T.F. (2005). Oxy-fuel combustion technology for coal-fired power generation. Progress in Energy and Combustion Science, 31(4): 283-307. https://doi.org/10.1016/j.pecs.2005.07.001

[7] Czakiert, T., Bis, Z., Muskala, W., Nowak, W. (2006). Fuel conversion from oxy-fuel combustion in a circulating fluidized bed. Fuel Processing Technology, 87(6): 531-538. https://doi.org/10.1016/j.fuproc.2005.12.003

[8] Gu, J., Shao, Y., Zhong, W. (2019). Study on oxy-fuel combustion behaviors in a S-CO_2 CFB by 3D CFD simulation. Chemical Engineering Science, 211: 115262. https://doi.org/10.1016/j.ces.2019.115262

[9] Abbass, A. (2025). Advanced zero-emission power cycles: Integration of Graz cycle, high-temperature steam cycle, and partial oxidation gas turbines for hydrogen-based, carbon-neutral, and high-efficiency power generation. International Journal of Progressive Research in Engineering Management and Science, 5(3): 802-815. https://doi.org/10.58257/IJPREMS39028

[10] Abbass, A. (2025). Comprehensive review of combustion stability and instabilities in premixed systems. International Journal of Progressive Research in Engineering Management and Science, 5(3): 1174-1184. https://doi.org/10.58257/IJPREMS39088

[11] Liu, C., Huang, Y., Wang, X., Zhu, Z., Yu, M., Bu, C., Zhang, J. (2021). Interactions of $PbCl_2$ capture and $CdCl_2$ capture by kaolin in the high-temperature $PbCl_2$-$CdCl_2$-Kaolin reaction system. Fuel, 286: 119346. https://doi.org/10.1016/j.fuel.2020.119346

[12] Nemitallah, M.A., Habib, M.A., Badr, H.M., Said, S.A., et al. (2017). Oxy-fuel combustion technology: Current status, applications, and trends. International Journal of Energy Research, 41(12): 1670-1708. https://doi.org/10.1002/er.3722

[13] Riaza, J., Gil, M.V., Álvarez, L., Pevida, C., Pis, J.J., Rubiera, F. (2012). Oxy-fuel combustion of coal and biomass blends. Energy, 41(1): 429-435. https://doi.org/10.1016/j.energy.2012.02.057

[14] Scheffknecht, G., Al-Makhadmeh, L., Schnell, U., Maier, J. (2011). Oxy-fuel coal combustion—A review of the current state-of-the-art. International Journal of Greenhouse Gas Control, 5: S16-S35. https://doi.org/10.1016/j.ijggc.2011.05.020

[15] Frassoldati, A., Cuoci, A., Faravelli, T., Ranzi, E., Candusso, C., Tolazzi, D. (2009). Simplified kinetic schemes for oxy-fuel combustion. In 1st International Conference on Sustainable Fossil Fuels for Future Energy–S4FE 2009, pp. 1-14. https://chemistry.cerfacs.fr/wp-content/uploads/sites/76/2018/08/Frassoldati_full-paper.pdf.

[16] Wang, J.H., Pan, S.C., Hu, X.Y., Adams, N.A. (2019). A split random time-stepping method for stiff and nonstiff detonation capturing. Combustion and Flame, 204: 397-413. https://doi.org/10.1016/j.combustflame.2019.03.034

[17] Liu, C.Y., Chen, G., Sipöcz, N., Assadi, M., Bai, X.S. (2012). Characteristics of oxy-fuel combustion in gas turbines. Applied Energy, 89(1): 387-394. https://doi.org/10.1016/j.apenergy.2011.08.004

[18] Krieger, G.C., Campos, A.P.V., Takehara, M.D.B., Da Cunha, F.A., Veras, C.G. (2015). Numerical simulation of oxy-fuel combustion for gas turbine applications. Applied Thermal Engineering, 78: 471-481. https://doi.org/10.1016/j.applthermaleng.2015.01.001

[19] Saanum, I., Ditaranto, M. (2017). Experimental study of oxy-fuel combustion under gas turbine conditions. Energy and Fuels, 31(4): 4445-4451. https://doi.org/10.1021/acs.energyfuels.6b03114

[20] Toftegaard, M.B., Brix, J., Jensen, P.A., Glarborg, P., Jensen, A.D. (2010). Oxy-fuel combustion of solid fuels. Progress in Energy and Combustion Science, 36(5): 581-625. https://doi.org/10.1016/j.pecs.2010.02.001

[21] Díaz Velázquez, H., Cerón-Camacho, R., Mosqueira-Mondragón, M.L., Hernández-Cortez, J.G., Montoya de la Fuente, J.A., Hernández-Pichardo, M.L., Beltrán-Oviedo, T.A., Martínez-Palou, R. (2022). Recent progress on catalyst technologies for high quality gasoline production. Catalysis Reviews, 65(4): 1079-1299. https://doi.org/10.1080/01614940.2021.2003084

[22] Shakeel, M.R., Sanusi, Y.S., Mokheimer, E.M.A. (2018). Numerical modeling of oxy-methane combustion in a model gas turbine combustor. Applied Energy, 228: 68-81. https://doi.org/10.1016/j.apenergy.2018.06.071

[23] Yin, C., Rosendahl, L., Kær, S.K. (2011). Modelling of radiation heat transfer in oxy-fuel combustion systems. Fuel, 90(7): 2519-2529. https://doi.org/10.1016/j.fuel.2011.03.023

[24] Yin, C., Yan, J. (2016). Oxy-fuel combustion of pulverized fuels: Combustion fundamentals and modeling. Applied Energy, 162: 742-762. https://doi.org/10.1016/j.apenergy.2015.10.149

[25] Li, B., Shi, B., Zhao, X., Ma, K., Xie, D., Zhao, D, Li, J. (2018). Oxy-fuel combustion of methane in a swirl tubular flame burner under various oxygen contents: Operation limits and combustion instability. Experimental Thermal and Fluid Science, 90: 115-124. https://doi.org/10.1016/j.expthermflusci.2017.09.001